

Rapid Evaluation of Tyrosine Kinase Activity of Membrane-Integrated Human Epidermal Growth Factor Receptor Using the Yeast $G\gamma$ Recruitment System

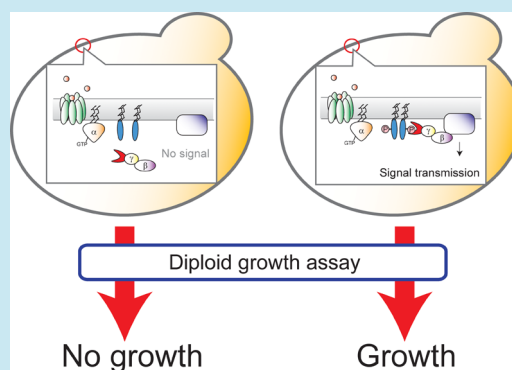
Nobuo Fukuda and Shinya Honda*

Biomedical Research Institute, National Institute of Advanced Industrial Science and Technology (AIST), Higashi, Tsukuba, Ibaraki 305-8566, Japan

S Supporting Information

ABSTRACT: Epidermal growth factor receptor (EGFR) is a member of the receptor tyrosine kinase family and plays key roles in the regulation of fundamental cellular processes, including cell proliferation, migration, differentiation, and survival. Deregulation of EGFR tyrosine kinase activity is involved in the development and progression of human cancers. In the present study, we attempted to develop a method to evaluate the tyrosine kinase activity of human EGFR using the yeast $G\gamma$ recruitment system. Autophosphorylation of tyrosine residues on the cytoplasmic tail of EGFR induces recruitment of Grb2-fused $G\gamma$ subunits to the inner leaflet of the plasma membrane in yeast cells, which leads to G-protein signal transduction and activation of downstream signaling events, including mating and diploid cell growth. We demonstrate that our system is applicable for the evaluation of tyrosine kinase inhibitors, which are regarded as promising drug candidates to prevent the growth of tumor cells. This approach provides a rapid and easy-to-use tool to select EGFR-targeting tyrosine kinase inhibitors that are able to permeate eukaryotic membranes and function in intracellular environments.

KEYWORDS: tyrosine kinase, epidermal growth factor receptor, yeast, $G\gamma$ recruitment system, inhibitor screening



Receptor tyrosine kinases (RTK) are involved in intercellular signal transduction events that regulate cell growth, migration, proliferation, and differentiation. RTK dimerization is induced by the binding of extracellular ligands and is followed by the autophosphorylation of tyrosine residues, which serve as docking sites for signal transduction molecules containing Src-homology 2 (SH2) and phosphotyrosine binding (PTB) domains, leading to the activation of downstream signaling events.^{1,2}

Epidermal growth factor receptor (EGFR) is a member of the RTK family and plays essential roles in both normal and oncogenic signaling pathways.³ In normal cells, EGFR is activated by binding of the epidermal growth factor (EGF) to the extracellular domain (Figure 1A). However, aberrational activations of EGFR resulting from its overexpression and/or activating mutations^{4,5} are associated with a variety of human cancers. Therefore, human EGFR is regarded as an important therapeutic target in the field of oncology.

One approach to suppress aberrant signal transduction triggered by EGFR activation is treatment with small-molecule drugs that inhibit tyrosine kinase activity and thereby block receptor autophosphorylation.^{6–9} For example, gefitinib and erlotinib are small-molecule tyrosine kinase inhibitors (TKI) that are widely used as anticancer drugs, particularly against nonsmall cell lung cancer. Due to their low toxicity and good

efficacy, the identification of TKI targeting human EGFR has attracted considerable attention for anticancer therapy.¹⁰

Several biochemical^{11,12} and cell-based assays^{13,14} have been developed to screen for TKI from compound libraries. Among these assays, the yeast *Saccharomyces cerevisiae* represents an inexpensive and tractable heterologous system for measuring the tyrosine kinase activity of EGFR in a eukaryotic cellular environment. Due to the absence of endogenous RTK, yeast provides a null background for measured the expression and activity of endogenous RTK.⁹ Recently, the Sos- and Ras-recruitment systems (SRS and RRS, respectively), which are yeast two-hybrid systems based on the Ras signaling pathway,¹⁵ were applied to measuring inhibition of the tyrosine kinase activity of EGFR by specific inhibitors.^{9,16} Notably, however, the growth rate of yeast in SRS or RRS is markedly slower than that found in other growth assays using yeast cells.¹⁷ Due to this limitation, these assays require at least 1 week to screen for TKI.

To establish a method that allows for the rapid evaluation of EGFR tyrosine kinase activity, we adopted the $G\gamma$ recruitment system (GRS), which utilizes the yeast G-protein signaling pathway.^{17–20} In this system, activation of the G-protein signaling pathway by the tyrosine kinase activity of exogenous

Received: February 24, 2014

Published: July 9, 2014

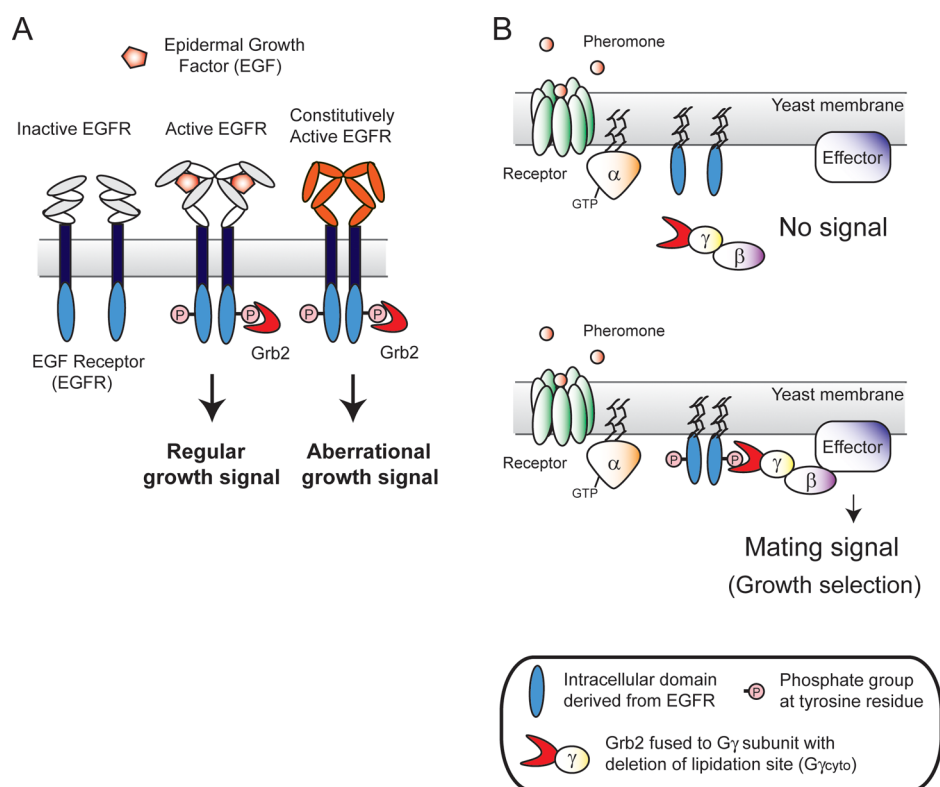


Figure 1. Evaluation of tyrosine kinase activity of human EGFR by utilizing yeast G-protein signal transduction. (A) Schematic illustration of the role of EGFR in human cells. EGF-induced dimerization leads to autophosphorylation of EGFR through its own tyrosine kinase activity, resulting in signal transmission regulating cell growth. In contrast, constitutively active EGFR transmits growth signals without restriction and is involved in the development and progression of human cancers. (B) Schematic illustration of the proposed system for evaluation of tyrosine kinase activity of human EGFR. Wild-type $G\gamma$ is lipid-modified at the C-terminus and localizes to the plasma membrane to transmit the intracellular signal. Engineered $G\gamma$ lacking membrane association ($G\gamma_{cyto}$) is fused to Grb2. When the intracellular domain derived from EGFR ($EGFR_{cyto}$) is not phosphorylated, G-protein signaling is not restored because Grb2- $G\gamma_{cyto}$ does not localize to the membrane. However, when $EGFR_{cyto}$ is phosphorylated by its tyrosine kinase activity, Grb2- $G\gamma_{cyto}$ localizes to the plasma membrane, leading to the restoration of G-protein signaling and induction of the mating response and generation of diploid cells.

human EGFR integrated on yeast cell membrane results in diploid formation and cell growth (Figure 1B). In this present study, we examined the feasibility and potential of this system as a primary screening tool for identifying TKI targeting human EGFR.

RESULTS AND DISCUSSION

General Strategy for Assaying EGFR Tyrosine Kinase Activity. An outline of the experimental design, which was based on components of the G-protein signaling pathway and used for the evaluation of tyrosine kinase activity of EGFR, is shown in Figure 1B. In this pathway, pheromone stimulation leads to activation of heterotrimeric G-proteins comprised of Gpa1 ($G\alpha$), Ste4 ($G\beta$), and Ste18 ($G\gamma$) proteins through the G-protein-coupled receptor. Once activated, G-proteins dissociate into $G\alpha$ subunits and $G\beta\gamma$ complexes, which then interact through $G\beta$ with effector molecules anchored in the plasma membrane, leading to activation of downstream signaling. Because yeast G-protein signaling requires localization of $G\gamma$ to the inner leaflet of the plasma membrane, such signaling is completely disrupted in $G\gamma$ mutants lacking lipidation sites ($G\gamma_{cyto}$).

To modify this system for the measurement of EGFR tyrosine kinase activity, the intracellular domain of EGFR ($EGFR_{cyto}$), which contains a tyrosine kinase domain and tyrosine phosphorylation sites, and Grb2, which contains a SH2 domain,

fused to $G\gamma_{cyto}$ (Grb2- $G\gamma_{cyto}$) were coexpressed in a strain lacking endogenous $G\gamma$ (*ste18 Δ*). In the absence of autophosphorylated tyrosine residues in plasma-membrane anchored $EGFR_{cyto}$, Grb2- $G\gamma_{cyto}$ does not associate with $EGFR_{cyto}$ and remains in the cytosol. In contrast, autophosphorylation of $EGFR_{cyto}$ induces recruitment of Grb2- $G\gamma_{cyto}$ to the plasma membrane and restores G-protein signal transduction, leading to diploid cell formation (mating). Thus, by performing a diploid growth assay, the tyrosine kinase activity of EGFR can be evaluated in this system.

Investigation of Acceptable Distance Between $G\gamma_{cyto}$ and Plasma Membrane for G-Protein Signaling. To link EGFR tyrosine kinase activity with G-protein signaling, $G\beta$ must interact with the effector molecule anchored in the plasma membrane when Grb2- $G\gamma_{cyto}$ binds to autophosphorylated $EGFR_{cyto}$ (Figure 1B). As shown in Figure 2A, $EGFR_{cyto}$ consists of 541 amino-acid residues (aa), whereas $G\gamma_{cyto}$ consists of 105 aa. Due to its large size, it was considered that $EGFR_{cyto}$ may sterically hinder the accessibility of the $G\beta\gamma_{cyto}$ complex to the membrane-anchored effector molecule.

To assess this possibility, we prepared several $G\gamma_{cyto}$ - $EGFR_{cyto}$ fusion proteins (Figure 2A). The fusion proteins included an N-terminal 10-aa myristoylation and palmitoylation (MP) sequence motif derived from Gpa1,²⁰ which allow for localization in the plasma membrane after dual lipidation. To determine the ideal distance between $G\gamma_{cyto}$ and the plasma

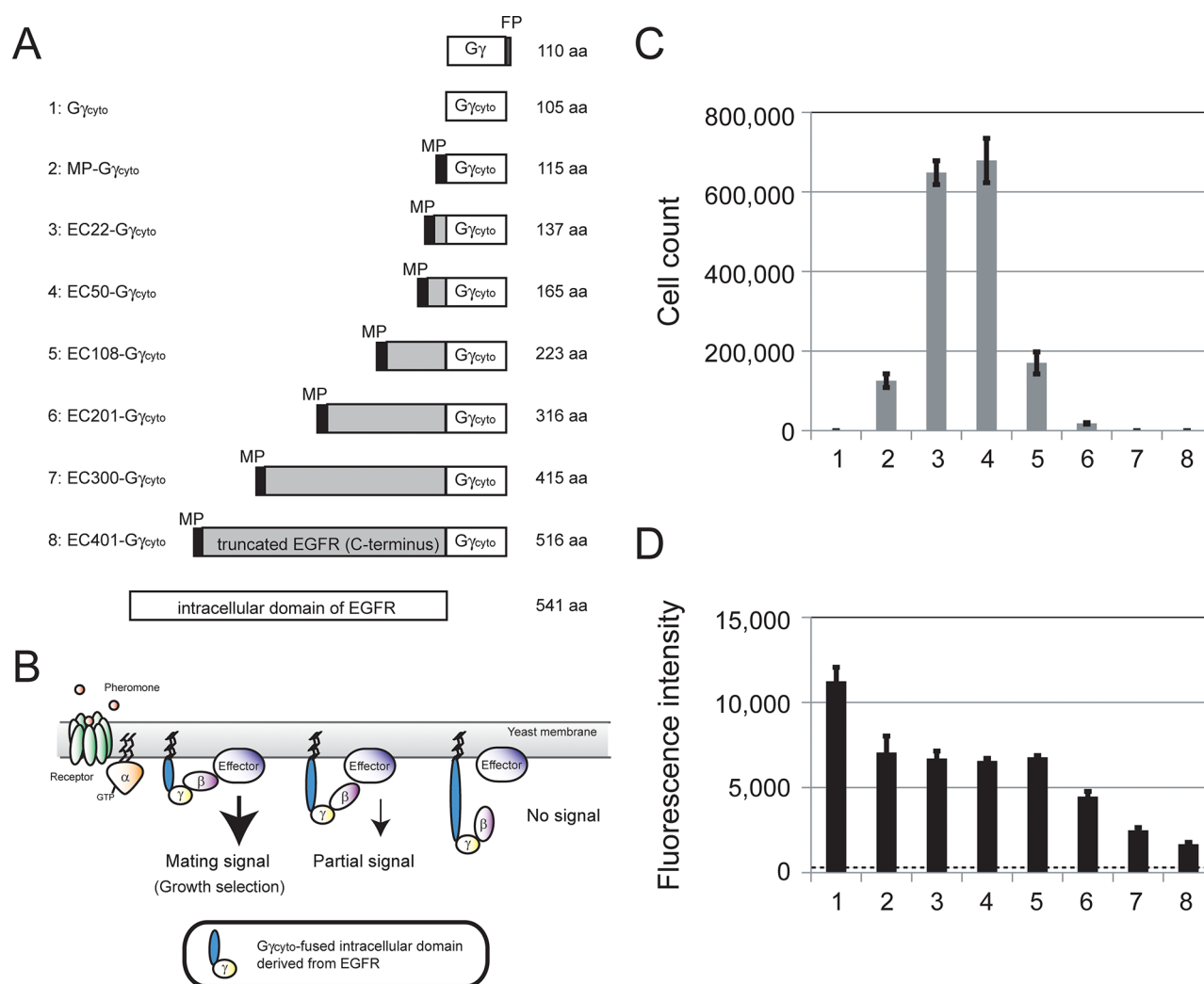


Figure 2. Expression of $EGFR_{cyto}$ - $G\gamma_{cyto}$ fusion proteins with an N-terminal motif for myristoylation and palmitoylation to investigate the acceptable distance between $G\gamma_{cyto}$ and plasma membrane to restore G-protein signaling. (A) Schematic representation of the fusion proteins constructed in this study. The N-terminal 10 aa derived from Gpa1 (yeast $G\alpha$ subunit), which receives dual lipid modification and confers membrane-targeting ability to the protein, was termed the MP sequence. Several truncated $EGFR_{cyto}$ of different lengths were inserted between MP and $G\gamma_{cyto}$. (B) Schematic illustration of the relationship between the location of $G\beta\gamma_{cyto}$ and restoration of G-protein signaling. With increasing length of the sequence inserted between MP and $G\gamma_{cyto}$, $G\beta\gamma_{cyto}$ would be located at increasing distance from the plasma membrane. (C) Cell count in the diploid growth assay to investigate the acceptable distance between $G\gamma_{cyto}$ and the plasma membrane to restore G-protein signaling. Values are presented as means \pm standard deviations from three independent experiments. The lane number corresponds to each protein described in A. (D) Fluorescent reporter assay to quantify the expression level of a GFP reporter fused to $G\gamma_{cyto}$. The dashed line indicates the level of autofluorescence of yeast cells. Values are presented as means \pm standard deviations from three independent experiments. The lanes correspond to those in C.

membrane based on the length of the inserted peptide sequence as an indicator, aa sequences of varying lengths derived from $EGFR_{cyto}$ were inserted between MP and $G\gamma_{cyto}$, as shown in Figures 2A and B.

The *ste18* Δ strain MCF-B1L (lacking endogenous $G\gamma$) was utilized as a host to express $G\gamma_{cyto}$ and $G\gamma_{cyto}$ -fused proteins (Figure 2A) using the plasmids shown in Table 1. Figure 2C shows the results of diploid growth assays performed using the transformant strains. Based on the results in the previous report,²⁰ $G\gamma_{cyto}$ and MP- $G\gamma_{cyto}$ were used as the negative and positive control, respectively. Expression of $G\gamma_{cyto}$ did not result in diploid formation, consistent with the impaired G-protein signaling caused by the lack of lipidation sites. In contrast, expression of MP- $G\gamma_{cyto}$, which localized to the plasma membrane, restored G-protein signaling, as evidenced by the production of diploid cells. As schematically illustrated in Figure 2B, the number of generated diploids varied according to the

length of the sequence inserted between MP and $G\gamma_{cyto}$. Fusion proteins EC22- and EC50- $G\gamma_{cyto}$ successfully restored G-protein signaling and led to the formation of approximately 6-fold more diploid cells than that formed by cells expressing MP- $G\gamma_{cyto}$. Although EC108- and EC201- $G\gamma_{cyto}$ also restored G-protein signaling, the diploid cell count markedly decreased with increasing length of the inserted $EGFR_{cyto}$ sequence. Neither EC300- nor EC401- $G\gamma_{cyto}$ restored signal transduction, as demonstrated by the lack of diploid cells.

To compare the expression levels of the $G\gamma_{cyto}$ -fused proteins, a GFP reporter was fused to the C-terminus of $G\gamma_{cyto}$. The fluorescence intensity of cell suspensions of yeast expressing each of the GFP-tagged $G\gamma_{cyto}$ -fused proteins was measured (Figure 2D). The fluorescence intensity measurements showed that although $G\gamma_{cyto}$ was synthesized at the highest level, all $G\gamma_{cyto}$ -fused proteins were also clearly expressed in yeast. Among the examined proteins, EC22-, EC50-, and EC108- $G\gamma_{cyto}$

Table 1. Yeast Strains and Plasmids Used in This Study

name	description	reference source
Yeast Strains		
BY4741	<i>MATα his3Δ1 ura3Δ0 leu2Δ0 met15Δ0</i>	<i>Yeast</i> (1998) 14, 115–132
BY4742	<i>MATα his3Δ1 ura3Δ0 leu2Δ0 lys2Δ0</i>	<i>Yeast</i> (1998) 14, 115–132
MCF-B1L	BY4741 <i>FIG1::FIG1-EGFP ste18Δ::LEU2</i>	<i>PLoS One</i> (2013) 26, e70100
B1L-GrG	MCF-B1L <i>his3::HIS3-P_{PGK1}-GRB2-Gγ_{cyto}-T_{ADH1}</i>	present study
B1U-GL	B1L-GrG <i>ste18Δ::URA3-P_{PGK1}-EGFR(LR)_{cyto}-T_{ADH1}</i>	present study
Plasmids		
pHY-PGA	2 μ ori, <i>HIS3</i> marker and <i>P_{PGK1}-EGFP</i>	<i>PLoS One</i> (2013) 26, e70100
pHY-G γ c	2 μ ori, <i>HIS3</i> marker and <i>P_{PGK1}-Gγ_{cyto}</i>	<i>PLoS One</i> (2013) 26, e70100
pHY-10YG γ c	2 μ ori, <i>HIS3</i> marker and <i>P_{PGK1}-MP-Gγ_{cyto}</i>	<i>PLoS One</i> (2013) 26, e70100
pHY-EC22-G γ c	2 μ ori, <i>HIS3</i> marker and <i>P_{PGK1}-EC22-Gγ_{cyto}</i>	present study
pHY-EC50-G γ c	2 μ ori, <i>HIS3</i> marker and <i>P_{PGK1}-EC50-Gγ_{cyto}</i>	present study
pHY-EC108-G γ c	2 μ ori, <i>HIS3</i> marker and <i>P_{PGK1}-EC108-Gγ_{cyto}</i>	present study
pHY-EC201-G γ c	2 μ ori, <i>HIS3</i> marker and <i>P_{PGK1}-EC201-Gγ_{cyto}</i>	present study
pHY-EC300-G γ c	2 μ ori, <i>HIS3</i> marker and <i>P_{PGK1}-EC300-Gγ_{cyto}</i>	present study
pHY-EC401-G γ c	2 μ ori, <i>HIS3</i> marker and <i>P_{PGK1}-EC401-Gγ_{cyto}</i>	present study
pHY-G γ cG	2 μ ori, <i>HIS3</i> marker and <i>P_{PGK1}-Gγ_{cyto}-EGFP</i>	<i>PLoS One</i> (2013) 26: e70100
pHY-10YG γ cG	2 μ ori, <i>HIS3</i> marker and <i>P_{PGK1}-MP-Gγ_{cyto}-EGFP</i>	<i>PLoS One</i> (2013) 26: e70100
pHY-EC22-G γ cG	2 μ ori, <i>HIS3</i> marker and <i>P_{PGK1}-EC22-Gγ_{cyto}-EGFP</i>	present study
pHY-EC50-G γ cG	2 μ ori, <i>HIS3</i> marker and <i>P_{PGK1}-EC50-Gγ_{cyto}-EGFP</i>	present study
pHY-EC108-G γ cG	2 μ ori, <i>HIS3</i> marker and <i>P_{PGK1}-EC108-Gγ_{cyto}-EGFP</i>	present study
pHY-EC201-G γ cG	2 μ ori, <i>HIS3</i> marker and <i>P_{PGK1}-EC201-Gγ_{cyto}-EGFP</i>	present study
pHY-EC300-G γ cG	2 μ ori, <i>HIS3</i> marker and <i>P_{PGK1}-EC300-Gγ_{cyto}-EGFP</i>	present study
pHY-EC401-G γ cG	2 μ ori, <i>HIS3</i> marker and <i>P_{PGK1}-EC401-Gγ_{cyto}-EGFP</i>	present study
pHY-GrG	2 μ ori, <i>HIS3</i> marker and <i>P_{PGK1}-GRB2-Gγ_{cyto}</i>	present study
pUY-PGA	2 μ ori, <i>URA3</i> marker and <i>P_{PGK1}-EGFP</i>	present study
pUY-EC-WT	2 μ ori, <i>URA3</i> marker and <i>P_{PGK1}-EGFR(WT)_{cyto}-FP</i>	present study
pUY-EC-LR	2 μ ori, <i>URA3</i> marker and <i>P_{PGK1}-EGFR(LR)_{cyto}-FP</i>	present study
pUY-EC-KA	2 μ ori, <i>URA3</i> marker and <i>P_{PGK1}-EGFR(KA)_{cyto}-FP</i>	present study

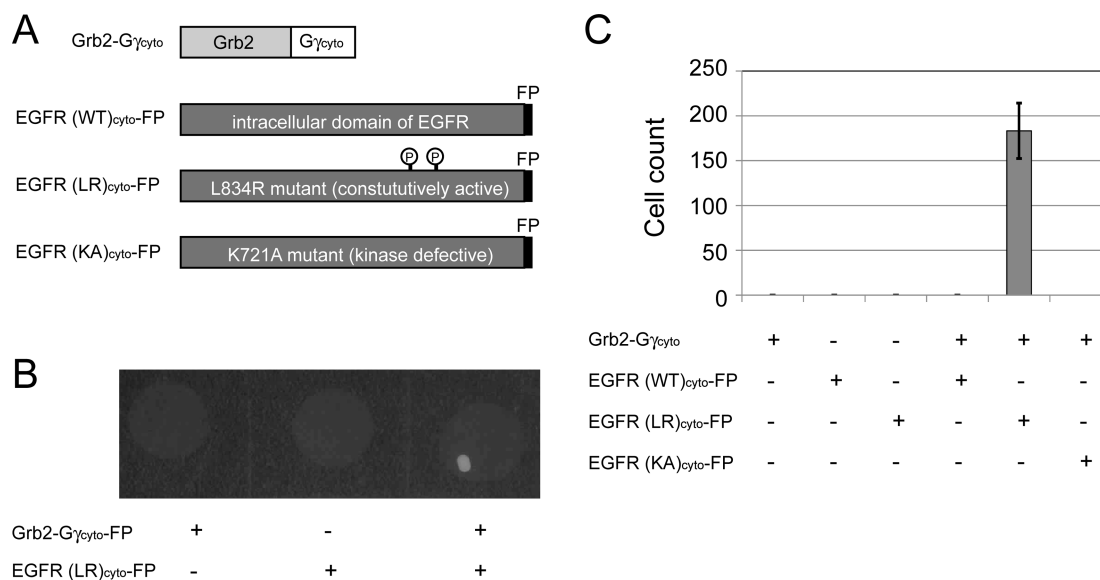


Figure 3. Restoration of G-protein signaling by the interaction between Grb2 and phosphorylated EGFR_{cyto}. (A) Schematic representation of the Grb2-G γ _{cyto} fusion protein and genetically modified EGFR_{cyto} proteins. The C-terminal 9 aa derived from Ste18 (yeast G γ subunit), which receives dual lipid modification (farnesylation and palmitoylation) and confers membrane-targeting ability to the protein, was termed the FP sequence and attached to the C-terminus of wild-type (WT), constitutively active (LR), and kinase defective (KA) EGFR_{cyto} proteins. (B) Images of colony formation in the diploid growth assay for strain MCF-B1L. Cell suspensions (10 μ L, OD₆₀₀ set at 1) were grown on selective solid medium and incubated for 2 days. (C) Cell count in the diploid growth assay for evaluation of tyrosine kinase activity of human EGFR. Values are presented as means \pm standard deviations from three independent experiments.

were expressed at a level equivalent to that of MP-G γ _{cyto}, whereas the levels of EC201-, EC300-, and EC401-G γ _{cyto} decreased with increasing length of the inserted sequence.

Notably, even though EC50-G γ _{cyto} was synthesized at an equivalent level to that of EC108-G γ _{cyto}, the diploid cell count substantially differed between the two G γ _{cyto}-fused proteins

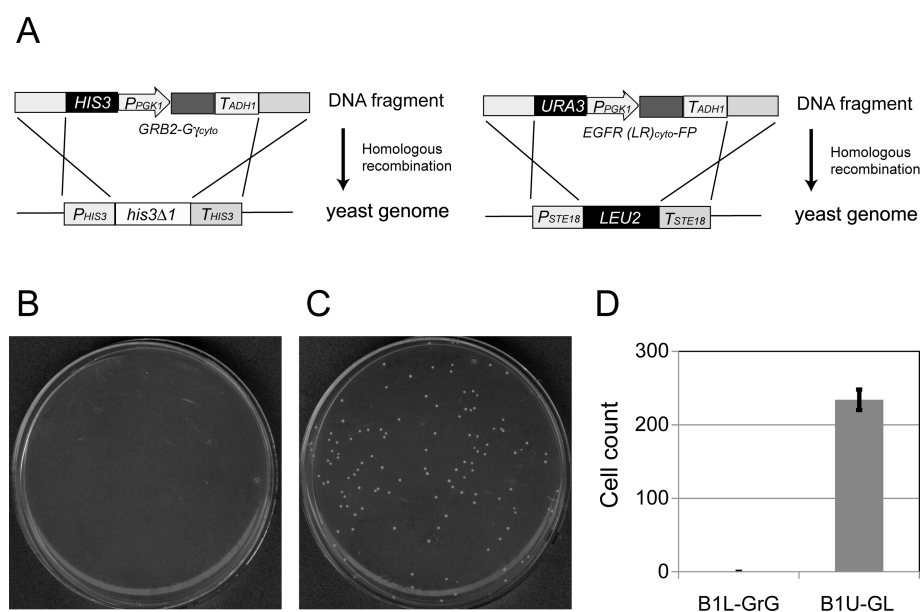


Figure 4. Construction of yeast strains with the Grb2- $G\gamma_{\text{cyto}}$ and/or EGFR (LR) $_{\text{cyto}}$ -FP coding genes integrated into the chromosomal DNA. (A) Schematic representation of the construction and chromosomal integration of the target genes. Strain MCF-B1L was used as the parental strain to yield strains B1L-GrG (expressing Grb2- $G\gamma_{\text{cyto}}$) and B1U-GL (expressing both Grb2- $G\gamma_{\text{cyto}}$ and EGFR (LR) $_{\text{cyto}}$ -FP). (B) Images of colony formation in the diploid growth assay for strain B1L-GrG. Cell suspensions (1 mL, OD_{600} set at 0.5) were spread on selective solid medium and incubated for 2 days. (C) Images of colony formation in the diploid growth assay for strain B1U-GL. Cell suspensions (1 mL, OD_{600} set at 0.5) were spread on selective solid medium and incubated for 2 days. (D) Quantitative cell count in the diploid growth assay after 8 h of cocultivation time. Values are presented as means \pm standard deviations from three independent experiments.

(Figure 2C). Together, these results indicate that the distance between $G\gamma_{\text{cyto}}$ and the plasma membrane significantly influences the efficiency of G-protein signaling. Specifically, spatial segregation of $G\gamma_{\text{cyto}}$ from the plasma membrane by greater than 300 aa appears to be unfavorable for G-protein signaling in the GRS.

Relocalization of Autophosphorylated Tyrosine Residues of EGFR $_{\text{cyto}}$ to the Plasma Membrane Using a C-Terminal Lipidation Motif. Autophosphorylated Tyr-1068 (Y1068) of EGFR has a crucial role in the recruitment of Grb2 to the plasma membrane²¹ and is located 423 aa from the N-terminus of EGFR $_{\text{cyto}}$, suggesting that $G\gamma_{\text{cyto}}$ would be segregated from the plasma membrane when Grb2- $G\gamma_{\text{cyto}}$ binds to EGFR $_{\text{cyto}}$. However, because Y1068 is located at aa position 119 when counted from the C-terminus of EGFR $_{\text{cyto}}$, this residue would be located closer to the plasma membrane if the C-terminus of EGFR $_{\text{cyto}}$ was anchored in the plasma membrane.

To restore G-protein signaling by locating Y1068 of EGFR $_{\text{cyto}}$ closer to the plasma membrane, we added a sequence motif (FP) consisting of the C-terminal 9 aa derived from Ste18¹⁷ for the attachment of palmitate and farnesyl groups to three types of EGFR $_{\text{cyto}}$ proteins: wild-type EGFR $_{\text{cyto}}$ (EGFR (WT) $_{\text{cyto}}$ -FP), EGFR $_{\text{cyto}}$ derived from an L834R mutant²² that is constitutively dimerized and activated even in the absence of EGF (EGFR (LR) $_{\text{cyto}}$ -FP), and a kinase-defective K721A mutant²³ (EGFR (KA) $_{\text{cyto}}$ -FP; Figure 3A). Strain MCF-B1L was utilized as a host to express Grb2- $G\gamma_{\text{cyto}}$ and/or the three EGFR $_{\text{cyto}}$ fusion proteins. Figure 3B shows the results of a diploid growth assay for the three examined transformant strains. Each cell suspension (10 μ L, OD_{600} set at 1) was grown on the same selective solid medium. As expected, expression of Grb2- $G\gamma_{\text{cyto}}$ did not result in diploid cell formation because it cannot associate with the plasma membrane, and EGFR (LR) $_{\text{cyto}}$ -FP

alone did not due to the lack of $G\gamma_{\text{cyto}}$. In contrast, EGFR (LR) $_{\text{cyto}}$ -FP restored G-protein signaling when coexpressed with Grb2- $G\gamma_{\text{cyto}}$. Moreover, Figure 3C shows the results of a quantitative diploid growth assay for the six examined transformant strains. Each cell suspension (1 mL, OD_{600} set at 0.5) was grown on an individual selective solid medium, and then, the number of diploid colonies was measured for quantitative comparison. Among the three EGFR $_{\text{cyto}}$ -FP proteins, only EGFR (LR) $_{\text{cyto}}$ -FP restored G-protein signaling when coexpressed with Grb2- $G\gamma_{\text{cyto}}$. Taken together, these results suggest that autophosphorylation of EGFR $_{\text{cyto}}$ induces both membrane-localization of Grb2- $G\gamma_{\text{cyto}}$ and interaction of $G\beta$ with the membrane-anchored effector molecule.

In the GRS-based assay developed here, diploid colonies were visible within 2 days of incubation. This period is dramatically shorter than the 7 days required for colony formation in the assay based on RRS.⁹ As expected, the use of GRS allowed for rapid evaluation of EGFR tyrosine kinase activity. Although slight autophosphorylation of full-length wild-type EGFR was previously reported when it was overexpressed without the addition of EGF in yeast using a high-copy plasmid (containing 2 μ ori),⁹ here, EGFR (WT) $_{\text{cyto}}$ -FP did not restore any detectable signal transduction when overexpressed using a high-copy plasmid. As it is possible that the extracellular domain may be important for dimerization of overexpressed EGFR, even in the absence of EGF, we selected EGFR (LR) $_{\text{cyto}}$ as the target for further evaluation of TKI using this system.

Integration of Genes Encoding Grb2- $G\gamma_{\text{cyto}}$ and EGFR (LR) $_{\text{cyto}}$ -FP into Yeast Chromosomal DNA to Improve Gene Stability. Although high-copy plasmids allow for high gene expression levels, they suffer from poor gene stability. In our system, the genes encoding Grb2- $G\gamma_{\text{cyto}}$ and EGFR (LR) $_{\text{cyto}}$ -FP must both be constitutively expressed in yeast cells for the accurate evaluation of tyrosine kinase activity. To improve the

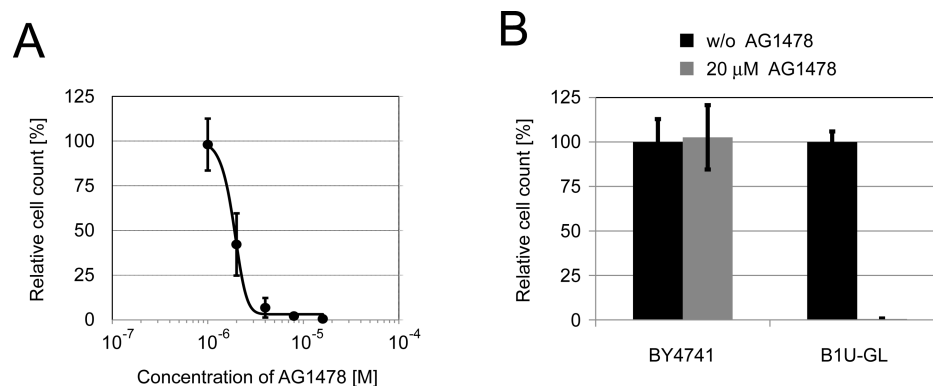


Figure 5. Inhibitory assay for AG1478. (A) Diploid cell counts in the inhibitory assay examining the dose-dependence of AG1478 in strain B1U-GL strain (expressing both Grb2- $G\gamma_{\text{cyto}}$ and EGFR (LR) $_{\text{cyto}}$ -FP). The cocultivation time with mating partner strain BY4742 was set at 8 h. Relative cell count was determined by dividing the diploid cell count with AG1478 treatment by that in medium without AG1478. (B) The diploid growth assay was performed with or without 20 μM AG1478 against strains BY4741 (expressing wild-type $G\gamma$) and B1U-GL. Relative cell count was determined by dividing the diploid cell count with AG1478 treatment by that in medium without AG1478, in order to investigate the inhibitory effect of AG1478 on EGFR (LR) $_{\text{cyto}}$ tyrosine kinase activity. Values are presented as means \pm standard deviations from three independent experiments.

gene stability of this system, we integrated these genes into the yeast chromosomal DNA of strain MCF-B1L, as shown in Figure 4A.

The diploid growth assay for the resulting strain, B1U-GL (expressing both Grb2- $G\gamma_{\text{cyto}}$ and EGFR (LR) $_{\text{cyto}}$ -FP), with the mating partner was performed after adjusting the cocultivation time (see Supporting Information Figure S1). Due to a decrease in the expression levels of Grb2- $G\gamma_{\text{cyto}}$ and EGFR (LR) $_{\text{cyto}}$ -FP, no diploid cells were generated after 1.5 h of cocultivation. However, the cell count markedly increased with increasing cocultivation time, and it was confirmed that the integrated genes were stably maintained in the yeast genome. Because long periods of cocultivation may facilitate excessive intracellular clearance of the added candidate compounds, we selected 8 h of cocultivation for the following evaluation of tyrosine kinase inhibition.

To confirm that no background colonies are formed after 8 h of cocultivation, we performed diploid growth assays for strains B1L-GrG (expresses Grb2- $G\gamma_{\text{cyto}}$) and B1U-GL (expresses both Grb2- $G\gamma_{\text{cyto}}$ and EGFR (LR) $_{\text{cyto}}$ -FP). No colonies grew on the solid selection medium in the case of strain B1L-GrG strain (Figure 4B), whereas numerous diploid colonies were formed by strain B1U-GL strain (Figure 4C). Figure 4D shows the quantitative comparison of the diploid cell count. These results suggest that adjustment of the cocultivation period can compensate for the lower expression levels of the Grb2- $G\gamma_{\text{cyto}}$ and EGFR (LR) $_{\text{cyto}}$ -FP genes upon chromosomal integration without background signals related to the restoration of G-protein signaling.

Evaluation of EGFR (LR) $_{\text{cyto}}$ Inhibitory Activity of AG1478. To validate the application of the described system for the identification of EGFR-specific TKI, we performed the inhibitory assay using the well-known small molecule EGFR inhibitor AG1478, which was expected to suppress the tyrosine kinase activity of EGFR (LR) $_{\text{cyto}}$. In the assay, AG1478 prevented generation of diploid cells in a dose-dependent manner (Figure 5A), and the addition of 16 μM AG1478 almost completely suppressed the tyrosine kinase activity of EGFR (LR) $_{\text{cyto}}$. The IC_{50} values of AG1478 for growth inhibition of human lung (A549) and prostate (DU145) cancer cell lines were approximately 1.2 μM in a previous report²⁴ and were estimated to be approximately 2 μM for EGFR in the present system. These results demonstrate that the effective concen-

tration for AG1478 was similar in yeast and human cell lines, and that the present system may be useful for the estimation of TKI activity in humans.

Although we confirmed that AG1478 had no toxic effects on yeast growth prior to conducting the inhibitory assay, this compound may act on endogenous components of the yeast G-protein signaling pathway. Therefore, we verified that AG1478 specifically prevents the interaction between EGFR and Grb2 by conducting an inhibitory assay with strains BY4741 (expressing wild-type $G\gamma$) and B1U-GL (expressing both Grb2- $G\gamma_{\text{cyto}}$ and EGFR (LR) $_{\text{cyto}}$ -FP) (Figure 5B). In contrast to strain BY4741, which formed an equivalent number of diploid cells in the presence and absence of AG1478, diploid formation by strain B1U-GL was nearly completely prevented by treatment with AG1478. These results strongly suggest that AG1478 acted on the exogenous components EGFR and Grb2.

To provide more evidence of the applicability of this approach, we conducted the inhibitory assay using another inhibitor; canertinib (see Supporting Information Figure S2). The IC_{50} values of canertinib for growth inhibition of human neuroblastoma cell lines were between 1.0 and 2.5 μM in a previous report.²⁵ In the current system, canertinib successfully exhibited inhibitory effect on EGFR kinase activity at almost the same level as AG1478. According to the result of inhibitory assay with strains BY4741 (expressing wild-type $G\gamma$), canertinib also acted on the exogenous components EGFR and Grb2. We propose that similar verification experiments would be effective in the primary screening of potential TKI candidates.

Conclusion. We have established a new approach to evaluate the tyrosine kinase activity of human EGFR and confirmed that this method may be useful as an exploration tool for identifying TKI. Use of the yeast G-protein signaling pathway allowed the construction of a rapid and tractable evaluation system that does not influence the growth rate of yeast cells. This system may be applicable for the identification of nontoxic EGFR inhibitors that are able to permeate the plasma membrane and stably function within the intracellular environment. The method developed here is also expected to promote further advances in the discovery of anticancer drugs.

Table 2. Sequences of Oligonucleotides Used to Construct Plasmids

no.	sequence
1	5'-aattggagctccaCCGCGGaaagatgccatttggcg-3'
2	5'-catgtcgacGCGGCCGcgtttatatttggtaaaa-3'
3	5'-atataaacGCGGCCGcatcgaccctccggagcgc-3'
4	5'-ccccagtttGGATCCtcatgctccaataattca-3'
5	5'-atataaacGCGGCCGcatggggtgtacagtgtacgcaacaataaggccacatcgctcg-3'
6	5'-ttgaactgatgtcattgctccaataattctgc-3'
7	5'-atgacatcagttcaaaactc-3'
8	5'-ccccagtttGGATCCttaaactatttggattgac-3'
9	5'-atataaacGCGGCCGcatggggtgtacagtgtacgcaacaataaggctccacagctgaaaatgc-3'
10	5'-atataaacGCGGCCGcatggggtgtacagtgtacgcaacaataaggcagcccaaatagcct-3'
11	5'-atataaacGCGGCCGcatggggtgtacagtgtacgcaacaataaggctctgtgagaaatcctgt-3'
12	5'-atataaacGCGGCCGcatggggtgtacagtgtacgcaacaataaggctgagcagcagta-3'
13	5'-atataaacGCGGCCGcatggggtgtacagtgtacgcaacaataaggatccaagcattatgacgc-3'
14	5'-atataaacGCGGCCGcatggggtgtacagtgtacgcaacaataaggctccagctacgtctca-3'
15	5'-tgtagccatGTCGACaactatttggattgac-3'
16	5'-atataaacGCGGCCGcatgagtgagaagctcccaacca-3'
17	5'-ccccagtttGGATCCtataagcgtacaacaactatttggctccaataattcactgc-3'
18	5'-tttggccgccccaaa-3'
19	5'-tttggccgccccaaa-3'
20	5'-taattccgcatagcagcgggaat-3'
21	5'-gctatcgcggaattaagagaagca-3'
22	5'-atataaacGCGGCCGcatggaagcctcccaaaa-3'
23	5'-cgtcaaacctgaggatgtcccccttt-3'
24	5'-catcctcaagtttgaacgaagaatgtga-3'
25	5'-ggatgtggtttcatttctat-3'
26	5'-gaaatgaaccacatcctggtttttggcaaaatc-3'
27	5'-gtttcaacttgacagagaggagaagt-3'
28	5'-tctctgtcaagtttggaaacgatgtgcagc-3'
29	5'-atgtcggctgtgtggcactgttctatgt-3'
30	5'-ggtgccacagcagccacatacgtccagc-3'
31	5'-ccccagtttGGATCCtagacgttccggttcacgg-3'
32	5'-ttgaactgatgtcatgacttccggttcacgggg-3'
33	5'-actactcgcactagagaaaaataataaagag-3'
34	5'-cctcaacaataACTAGTggagccataatgacagcag-3'
35	5'-ttatggctccACTAGTtattgtgagggtcagttat-3'
36	5'-tatagactatactgcttgccttctgttattctg-3'
37	5'-gaacgggcccCAGCTGttcaattcatctttttt-3'
38	5'-cgactcactatagggagaccggcagatgggtaataactgataaa-3'
39	5'-catagACTAGTatattatataatataatagg-3'
40	5'-ctccctatagtgatcgttaatttcgatGGATCCtcttagaattattgagaacg-3'
41	5'-gagaccggcagatCCGCGGggtaccCTCGAGtgatagtaataagaatcca-3'
42	5'-aatatACTAGTctatgttttgggtaccgaa-3'
43	5'-gagaccggcagatCCGCGGaaagatccgatttgggccc-3'
44	5'-attactatcaCTCGAGgagcagcctcatgctatacc-3'

METHODS

Strains and Media. Detailed information about *Saccharomyces cerevisiae* strains BY4741 and BY4742,²⁶ as well as the other strains used in this study, is shown in Table 1. Yeast cells were grown in YPD medium (1% yeast extract, 2% peptone, and 2% glucose) or SD medium (0.67% yeast nitrogen base without amino acids [Becton Dickinson and Company, Franklin Lakes, NJ, U.S.A.] and 2% glucose). Solid medium was prepared by adding 2% (w/v) agar.

Construction of Plasmids. The sequences of oligonucleotides used as PCR primers in this study are shown in Table 2. The plasmids listed in Table 1 were constructed as follows. Using pHY-PGA²⁰ as template, P_{PGK1} was amplified with oligonucleotide pair o1 and o2, and then inserted in place of P_{GAL1} at the *SacII-NotI* sites of pUY-GGA,²⁷ yielding plasmid

pUY-PGA. The *EGFR* gene was amplified from pco12-EGFR^{28–31} as template using oligonucleotide pair o3 and o4, and was then inserted into the *NotI-BamHI* sites of pUY-PGA, yielding plasmid pUY-EGFR-G.

The gene encoding the intracellular domain of EGFR ($EGFR_{cyto}$) was amplified with oligonucleotide pair o5 and o6 using pUY-EGFR-G as template. The gene encoding the $G\gamma$ mutant lacking membrane association ($G\gamma_{cyto}$) was amplified with oligonucleotide pair o7 and o8, using pHY- $G\gamma c^{20}$ as template. The amplified $EGFR_{cyto}$ and $G\gamma_{cyto}$ genes were then inserted in place of the *EGFP* gene at the *NotI-BamHI* sites of pUY-PGA, yielding plasmid pUY-EC- $G\gamma c$.

DNA fragments amplified from pUY-EC- $G\gamma c$ as template with oligonucleotide pairs o9 and o8, o10 and o8, o11 and o8, o12 and o8, o13 and o8, and o14 and o8 were inserted in place

of the *EGFP* gene at the *NotI*-*Bam*HI sites of pHY- PGA, yielding plasmids pHY-EC22-*Gyc*, pHY-EC50-*Gyc*, pHY-EC108-*Gyc*, pHY-EC201-*Gyc*, pHY-EC300-*Gyc*, and pHY-EC401-*Gyc*, respectively. For expression analyses, DNA fragments amplified with oligonucleotide pairs o9 and o15, o10 and o15, o11 and o15, o12 and o15, o13 and o15, and o14 and o15 using pUY-EC-*Gyc* as template were inserted into the *NotI*-*Sall* sites of pHY- PGA, yielding plasmids pHY-EC22-*GycG*, pHY-EC50-*GycG*, pHY-EC108-*GycG*, pHY-EC201-*GycG*, pHY-EC300-*GycG*, and pHY-EC401-*GycG*, respectively.

The plasmids used to express the *EGFR*_{cyto} and *GRB2*-*Gyc*_{cyto} genes were constructed as follows. The *EGFR*_{cyto} gene was amplified from pUY-EC-*Gyc* as template with oligonucleotide pair o16 and o17, and then inserted in place of the *EGFP* gene at the *NotI*-*Bam*HI sites of pUY- PGA, yielding plasmid pUY-EC-WT. DNA fragments amplified from pUY-EC-WT with oligonucleotide pairs o16 and o18, and o19 and o17 were inserted in place of the *EGFP* gene at the *NotI*-*Bam*HI sites of pUY- PGA, yielding plasmid pUY-EC-LR. Similarly, the DNA fragments amplified from pUY-EC-WT with oligonucleotide pairs o16 and o20, and o21 and o17 were inserted in place of the *EGFP* gene at the *NotI*-*Bam*HI sites of pUY- PGA, yielding plasmid pUY-EC-KA. Next, five DNA fragments were amplified from human genomic DNA (Roche Diagnostics K.K., Tokyo, Japan) using oligonucleotide pairs o22 and o23, o24 and o25, o26 and o27, o28 and o29, and o30 and o31, respectively, and were then inserted in place of the *EGFP* gene at the *NotI*-*Bam*HI sites of pHY- PGA, yielding plasmid pHY-Grb2. To construct a plasmid for the expression of *GRB2*-*Gyc*_{cyto}, the *GRB2* gene was amplified with oligonucleotide pair o22 and o32 using pHY-Grb2 as a template, and the *Gyc*_{cyto} gene was amplified with oligonucleotide pair o7 and o8 using pHY-*Gyc* as a template. The amplified *GRB2* and *Gyc*_{cyto} genes were then inserted in place of the *EGFP* gene at the *NotI*-*Bam*HI sites of pHY- PGA, yielding plasmid pHY-GrG.

The plasmids used for integration of the *EGFR*_{cyto} and *GRB2*-*Gyc*_{cyto} gene into yeast chromosomal DNA were constructed as follows. *T*_{HIS3} and *P*_{HIS3} were amplified from BY4741 genomic DNA using oligonucleotide pairs o33 and o34, and o35 and o36, respectively, and inserted in place of 2 μ ori at the *Spe*I sites of pHY- GrG, yielding plasmid pHY-GrG-Hpt. Next, the *URA3* selection marker gene was amplified from pUY-PGA as template using oligonucleotide pair o37 and o38. *P*_{STE18} and *T*_{STE18} were amplified from BY4741 genomic DNA using oligonucleotide pairs o39 and o40, and o41 and o42, respectively. The amplified *URA3*, *P*_{STE18}, and *T*_{STE18} fragments were inserted in place of the *kanMX4* selection marker gene at the *Pvu*II-*Sac*II sites of pK6,²⁷ yielding plasmid pUG-USpt. DNA fragments containing *P*_{PGK1}-*EGFR*(*LR*)_{cyto}-*T*_{ADH1} were amplified from pUY-EC-LR using oligonucleotide pair o43 and o44, and then inserted into the *Xho*I-*Sac*II sites of pUG-USpt, yielding plasmid pUG-USpt-LR. Each plasmid was introduced into yeast cells using the lithium acetate method.³²

Construction of Yeast Strains. The yeast strains constructed in this study are listed in Table 1. All DNA fragments were introduced into yeast cells using the lithium acetate method.³² DNA fragments containing *P*_{PGK1}-*GRB2*-*Gyc*_{cyto}-*T*_{ADH1} were prepared by digesting pHY-GrG-Hpt with *Spe*I, and were used to transform strain MCF-B1L. Transformants were selected on solid SD medium lacking histidine, yielding strain B1L-GrG.

DNA fragments containing *P*_{PGK1}-*EGFR*(*LR*)_{cyto}-*T*_{ADH1} were prepared by digesting pUG-USpt-LR with *Spe*I, and were then

used to transform strain B1L-GrG. Transformants were selected on YPD solid medium containing 500 μ g/mL G418, yielding strain B1U-GL.

Fluorescent Reporter Assay. The *EGFP* gene was fused to the C-terminus of *Gyc*_{cyto} and used as a fluorescent reporter of *Gyc*_{cyto}-fused hybrid protein expression in yeast cells. Cells were incubated in SD-His medium at 30 °C for 18 h, harvested, washed with distilled water, and then resuspended in 100 μ L distilled water to an optical density of 5.0 at 600 nm (OD_{600} = 5.0). GFP fluorescence intensity was measured using an Infinite 200 fluorescence microplate reader (Tecan Japan Co., Ltd., Kawasaki, Japan) at an excitation wavelength of 485 nm (20 nm bandwidth), emission wavelength of 535 nm (25 nm bandwidth) the a gain of 50.

Diploid Growth Assay. Evaluation of mating ability was performed as follows. Each engineered yeast strain was cultivated in 1 mL YPD medium with BY4742 as a mating partner at 30 °C for 1.5 h. The initial OD_{600} of each haploid strain was 0.1. After cultivation, cells were harvested, washed once in distilled water, and resuspended in distilled water. Using the appropriate dilution factor, which was determined based on OD_{600} , the cell suspensions were spread on SD plates without methionine and lysine, but supplemented 20 mg/L, histidine, 30 mg/L leucine, and 20 mg/L uracil (SD-Met, Lys plate) for the selection of diploid cells. After incubation at 30 °C for 2 days, the number of colonies formed by each strain were counted and multiplied by the respective dilution factor to estimate the number of diploid cells generated in an equivalent volume (1 mL) of cell suspension with an OD_{600} of 1.0. Image data of diploid colonies generated on the SD-Met, Lys plate were also recorded.

Evaluation of Tyrosine Kinase Inhibition. Each *MATa* strain was grown in 1 mL YPD medium containing 20 μ M *EGFR* kinase inhibitor AG1478 (Wako Pure Chemical Industries, Ltd., Osaka, Japan) or 5 μ M canertinib (AdooQ Bioscience, LLC., CA, U.S.A.) with strain BY4742 as a mating partner at 30 °C for 8 h. The initial OD_{600} of each haploid strain was 0.1. After cultivation, cells were harvested, washed once in distilled water, and resuspended in distilled water. Cell suspensions of each strain were spread on SD-Met, Lys plates using the appropriate dilution factor, which was determined based on OD_{600} . After incubation at 30 °C for 2 days, the number of colonies formed by each strain was counted and multiplied by the respective dilution factor to estimate the number of diploid cells generated in an equivalent volume (1 mL) of cell suspension with an OD_{600} of 1.0. The relative cell count for each strain was determined by dividing the diploid cell count by that in medium without AG1478.

■ ASSOCIATED CONTENT

📄 Supporting Information

This material is available free of charge via the Internet at <http://pubs.acs.org>.

■ AUTHOR INFORMATION

Corresponding Author

*Tel: +81 29 861 9444. Fax: +81 29 861 6194. Email: s.honda@aist.go.jp.

Author Contributions

N.F. designed the study, conducted experiments, analyzed data, and cowrote the manuscript. S.H. analyzed data and cowrote the manuscript. All authors read and approved the final manuscript.

Notes

The authors declare the following competing financial interest(s): We declare that all authors are inventors on a pending patent related to aspects of this system.

ACKNOWLEDGMENTS

Plasmid pco12-EGFR was provided by RIKEN BRC, which is a participating member of the National BioResource Project (NBRP) of the Ministry of Education, Culture, Sports, Science, and Technology (MEXT), Japan. This work was supported by Japan Society for the Promotion of Science (JSPS) KAKENHI (Grant Numbers 23860074 and 25820406).

ABBREVIATIONS

aa, amino-acid residues; EGF, epidermal growth factor; EGFR, epidermal growth factor receptor; EGFP, enhanced green fluorescent protein; GRS, $G\gamma$ recruitment system; PTB domain, phosphotyrosine binding domain; RRS, Ras-recruitment system; RTK, receptor tyrosine kinase; SH2 domain, Src-homology 2 domain; SRS, Sos-recruitment system; TKI, tyrosine kinase inhibitor

REFERENCES

- (1) Pawson, T. (1995) Protein modules and signalling networks. *Nature* 373, 573–580.
- (2) Gunde, T., and Barberis, A. (2005) Yeast growth selection system for detecting activity and inhibition of dimerization-dependent receptor tyrosine kinase. *Biotechniques* 39, 541–549.
- (3) Kim, Y., Li, Z., Apetri, M., Luo, B., Settleman, J. E., and Anderson, K. S. (2012) Temporal resolution of autophosphorylation for normal and oncogenic forms of EGFR and differential effects of gefitinib. *Biochemistry* 51, 5212–5222.
- (4) Paez, J. G., Janne, P. A., Lee, J. C., Tracy, S., Greulich, H., Gabriel, S., Herman, P., Kaye, F. J., Lindeman, N., Boggon, T. J., Naoki, K., Sasaki, H., Fujii, Y., Eck, M. J., Sellers, W. R., Johnson, B. E., and Meyerson, M. (2004) EGFR mutations in lung cancer: Correlation with clinical response to gefitinib therapy. *Science* 304, 1497–1500.
- (5) Lynch, T. J., Bell, D. W., Sordella, R., Gurubhagavatula, S., Okimoto, R. A., Brannigan, B. W., Harris, P. L., Haserlat, S. M., Supko, J. G., Haluska, F. G., Louis, D. N., Christiani, D. C., Settleman, J., and Haber, D. A. (2004) Activating mutations in the epidermal growth factor receptor underlying responsiveness of non-small-cell lung cancer to gefitinib. *N. Engl. J. Med.* 350, 2129–2139.
- (6) Levitzki, A. (1999) Protein tyrosine kinase inhibitors as novel therapeutic agents. *Pharmacol. Ther.* 82, 231–239.
- (7) Cohen, P. (2002) Protein kinases—The major drug targets of the twenty-first century? *Nat. Rev. Drug Discovery* 1, 309–315.
- (8) Fabbro, D., Parkinson, D., and Matter, A. (2002) Protein tyrosine kinase inhibitors: New treatment modalities? *Curr. Opin. Pharmacol.* 2, 374–381.
- (9) Gunde, T., and Barberis, A. (2005) Yeast growth selection system for detecting activity and inhibition of dimerization-dependent receptor tyrosine kinase. *Biotechniques* 39, 541–549.
- (10) Chen, X., Liu, Y., Røe, O. D., Qian, Y., Guo, R., Zhu, L., Yin, Y., and Shu, Y. (2013) Gefitinib or erlotinib as maintenance therapy in patients with advanced stage non-small cell lung cancer: A systematic review. *PLoS One* 8, e59314.
- (11) Zaman, G. J., Garritsen, A., de Boer, T., and van Boeckel, C. A. (2003) Fluorescence assays for high-throughput screening of protein kinases. *Comb. Chem. High Throughput Screen* 6, 313–320.
- (12) Minor, L. K. (2003) Assays to measure the activation of membrane tyrosine kinase receptors: Focus on cellular methods. *Curr. Opin. Drug Discovery Dev.* 6, 760–765.
- (13) Minor, L. K. (2003) Assays to measure the activation of membrane tyrosine kinase receptors: Focus on cellular methods. *Curr. Opin. Drug Discovery Dev.* 6, 760–765.

(14) Sims, C. E., and Allbritton, N. L. (2003) Single-cell kinase assays: Opening a window onto cell behavior. *Curr. Opin. Biotechnol.* 14, 23–28.

(15) Broder, Y. C., Katz, S., and Aronheim, A. (1998) The ras recruitment system, a novel approach to the study of protein–protein interactions. *Curr. Biol.* 8, 1121–1124.

(16) Busti, S., Sacco, E., Martegani, E., and Vanoni, M. (2008) Functional coupling of the mammalian EGF receptor to the Ras/cAMP pathway in the yeast *Saccharomyces cerevisiae*. *Curr. Genet.* 53, 153–162.

(17) Fukuda, N., Ishii, J., Tanaka, T., Fukuda, H., and Kondo, A. (2009) Construction of a novel detection system for protein–protein interactions using yeast G-protein signaling. *FEBS J.* 276, 2636–2644.

(18) Fukuda, N., Ishii, J., Tanaka, T., and Kondo, A. (2010) The competitor-introduced $G\gamma$ recruitment system, a new approach for screening affinity-enhanced proteins. *FEBS J.* 277, 1704–1712.

(19) Fukuda, N., Ishii, J., and Kondo, A. (2011) $G\gamma$ recruitment system incorporating a novel signal amplification circuit to screen transient protein–protein interactions. *FEBS J.* 278, 3086–3094.

(20) Fukuda, N., Doi, M., and Honda, S. (2013) Yeast one-hybrid $G\gamma$ recruitment system for identification of protein lipidation motifs. *PLoS One* 8, e70100.

(21) Rojas, M., Yao, S., and Lin, Y. Z. (1996) Controlling epidermal growth factor (EGF)-stimulated Ras activation in intact cells by a cell-permeable peptide mimicking phosphorylated EGF receptor. *J. Biol. Chem.* 271, 27456–27461.

(22) Zhang, X., Gureasko, J., Shen, K., Cole, P. A., and Kuriyan, J. (2006) An allosteric mechanism for activation of the kinase domain of epidermal growth factor receptor. *Cell.* 125, 1137–1149.

(23) Honegger, A. M., Kris, R. M., Ullrich, A., and Schlessinger, J. (1989) Evidence that autophosphorylation of solubilized receptors for epidermal growth factor is mediated by intermolecular cross-phosphorylation. *Proc. Natl. Acad. Sci. U. S. A.* 86, 925–929.

(24) Bojko, A., Reichert, K., Adamczyk, A., Ligeza, J., Ligeza, J., and Klein, A. (2012) The effect of tyrphostins AG494 and AG1478 on the autocrine growth regulation of A549 and DU145 cells. *Folia Histochem Cytobiol.* 50, 186–195.

(25) Richards, K. N., Zweidler-McKay, P. A., Van Roy, N., Speleman, F., Trevino, J., Zage, P. E., and Hughes, D. P. (2010) Signaling of ERBB receptor tyrosine kinases promotes neuroblastoma growth *in vitro* and *in vivo*. *Cancer* 116, 3233–3243.

(26) Brachmann, C. B., Davies, A., Cost, G. J., Caputo, E., Li, J., Hieter, P., and Boeke, J. D. (1998) Designer deletion strains derived from *Saccharomyces cerevisiae* S288C: A useful set of strains and plasmids for PCR-mediated gene disruption and other applications. *Yeast.* 14, 115–132.

(27) Fukuda, N., Matsukura, S., and Honda, S. (2013) Artificial conversion of the matingtype of *Saccharomyces cerevisiae* without autopolyploidization. *ACS Synth. Biol.* 2, 697–704.

(28) Velu, T. J., Beguinot, L., Vass, W. C., Zhang, K., Pastan, I., and Lowy, D. R. (1989) Retroviruses expressing different levels of the normal epidermal growth factor receptor: biological properties and new bioassay. *J. Cell Biochem.* 39, 153–166.

(29) Shigesada, K., Stark, G. R., Maley, J. A., Niswander, L. A., and Davidson, J. N. (1985) Construction of a cDNA to the hamster CAD gene and its application toward defining the domain for aspartate transcarbamylase. *Mol. Cell Biol.* 5, 1735–1742.

(30) Clark, A. J., Beguinot, L., Ishii, S., Ma, D. P., Roe, B. A., Merlino, G. T., and Pastan, I. (1986) Synthesis of epidermal growth factor (EGF) receptor *in vitro* using SP6 RNA polymerase-transcribed template mRNA. *Biochim. Biophys. Acta* 867, 244–251.

(31) Velu, T. J., Beguinot, L., Vass, W. C., Willingham, M. C., Merlino, G. T., Pastan, I., and Lowy, D. R. (1987) Epidermal-growth-factor-dependent transformation by a human EGF receptor proto-oncogene. *Science* 238, 1408–1410.

(32) Gietz, D., St. Jean, A., Woods, R. A., and Schiestl, R. H. (1992) Improved method for high efficiency transformation of intact yeast cells. *Nucleic Acids Res.* 20, 1425.